

2 Atmospheric Evolution and the History of Water on Mars

Helmut Lammer, Franck Selsis, Thomas Penz, Ute V. Amerstorfer,
Herbert I. M. Lichtenegger, Christoph Kolb and Ignasi Ribas

The discovery of high concentrations of water-ice just below the Martian surface in polar areas by the Mars Odyssey spacecraft has strengthened the debate about the possibility of life on Mars. Generally, it is believed that life on Earth emerged in liquid water through the processing of organic molecules. The possible origin of life on early Mars would have been related to the evolution of the planetary water inventory, so it is important to estimate the present amount of water-ice below the planetary surface.

There are also indications that large standing bodies of water ranging from lakes to an ocean may have existed in the past history of Mars. The high resolution altimetric data from the Mars Orbiter Laser Altimeter (MOLA) support this hypothesis since the flatness and smoothness of some surface areas suggest that they may have been part of the largest watershed on early Mars. Because present pressure conditions on the Martian surface prevent the formation of large amounts of stable liquid water, the atmosphere had to be much denser in the past.

In this second chapter we give an overview of all atmospheric loss processes related to the Martian water inventory during the planetary history. First, we show that XUV-driven hydrodynamic escape of hydrogen related to a more active young Sun may have affected the water inventory during the first few hundred Ma. Further, by using the observed atmospheric D/H ratio of the atmospheric water vapour on Mars, measured D/H ratios in SNC meteorites and D/H ratios related to the initial water source together with our atmospheric loss simulations, we estimate the present and early water-ice reservoirs which could exchange with the atmosphere, and discuss also the exobiologically relevant implications related to the incorporation of atmospheric oxygen to the Martian surface.

2.1 The First Billion Years

The Martian atmospheric history can be divided into early and late evolutionary periods [e.g., 1, 2, 3]. Early in the pre-3.5 Ga period, heavy noble gases like non-radiogenic Xe isotopes may have been hydrodynamically fractionated to their present composition, with corresponding depletions and fractionations of lighter primordial atmospheric species like deuterium (D) or H atoms [1]. Subsequently the CO₂ pressure history and the isotopic evolution of atmospheric species during this early period were dictated by the interplay of estimated losses with impact erosion, carbonate precipitation, additions by outgassing and carbonate recycling, and perhaps also by the feedback stabilisation under greenhouse conditions [1, 3]. The

second period is characterised by a uniform atmospheric loss to the present pressure of about 7 mbar, enhanced due to Mars' vanished intrinsic magnetic field and various non-thermal atmospheric escape processes.

2.1.1 The Source of Martian Water

There is much evidence from chemical and dynamical reasons that the source for the terrestrial crustal and surface water originated from planetary embryos, which have their origin in the asteroid belt [4]. This source is consistent with the isotopic record of the water content of the asteroid belt, by the chondrite record [5] and in the role of gas giants in clearing the asteroid belt [6]. The observed D/H ratio is consistent with the isotopic record of D/H in carbonaceous chondrites and terrestrial seawater (TSW) whose principal source is the asteroid belt.

The ratio of D/H isotopes of the water vapour in the current Martian atmosphere is about 5.2 times the terrestrial seawater value [7], where the cause for this difference is commonly assumed to be the isotopic fractionation during atmospheric escape of water, which can exchange with sources of water in the Martian crust and surface [7, 8]. Although the original D/H ratio in Martian water obtained from planetesimals is not well known, there are three known possibilities for the delivery of water to growing terrestrial planets, i.e. planetary embryos from beyond 2.5 AU, small asteroids from beyond 2.5 AU and comets from the Jovian orbital distance and beyond.

A recent study determined how much water on Mars could have been acquired from asteroid and comet populations [9]. By estimating the cumulative collision probability between asteroids and comets with Mars and by assuming that comets consist by about 50 % of water ice with a D/H ratio about twice the terrestrial value and that asteroids have about 10 wt. % water with D/H values comparable to the terrestrial ocean water value based on carbonaceous chondrites, it was found that Mars can acquire an amount of water equivalent to 6–27 % of the terrestrial oceans, with a D/H ratio of about 1.6 and 1.2 times the TSW ratio [9].

This study indicates that Mars actually received more water from small comets and asteroids with semi-major axes greater than 2.5 AU than the Earth, while the Earth may have received the bulk of its water from large embryos. By using this result one finds that the estimations of 6–27 % of the terrestrial oceans on Mars correspond to an equivalent global ocean depth of about 600 to 2700 m in the Martian crustal regolith and on the surface. (The water amount on Mars is often expressed in terms of the depth of a hypothetical ocean covering the entire Mars. Hereafter, we refer this simply to as the “equivalent depth”.) This is in agreement with previous studies [10, 11], where an outgassed amount with an equivalent depth of about 500 m on the Martian surface corresponds to a total accreted amount corresponding to 1000 m [9]. The D/H ratio of about 1.2 to 1.6 times the TSW ratio is below the average value of about 2.3 measured in Martian Shergotite meteorites [12], while an enrichment of about 1.6 times the TSW value is in

agreement with the D/H ratio measured in the 3.9 Ga old Martian meteorite ALH 84001.

The difference between the D/H ratio in the Shergottites and the asteroid-comet collision study can be interpreted as follows: either the D/H ratio in Martian meteorites was derived from magmatic water, which represents a primordial Martian value obtained from accretion of a mixture of asteroidal and cometary water or it was enhanced from the primordial value due to XUV-driven hydrodynamic escape caused by a more active young Sun [9, 12]. See also Chap. 1 by Baker et al. for the discussion of D/H ratios gathered from various Martian meteorites.

2.1.2 The Early Martian Atmosphere and the Radiation and Particle Environment of the Young Sun

Standard stellar evolutionary models constructed for the Sun show that the Zero-Age-Main-Sequence (ZAMS) Sun some 4.5 Ga ago was cooler by about 200 K and smaller by about 10 % than today, resulting in a luminosity of about 70 % of that of the present Sun. The lower luminosity of the young Sun should therefore have led to a much cooler surface temperature on early Earth and Mars, preventing a long-time stability of liquid water on the surface. In early studies of the variation of planetary climate due to the evolution of solar luminosity this problem became known as the “faint young Sun paradox” (FYSP) [14].

Later, a climate regulation model controlled by the CO₂ cycle was proposed [15], where CO₂ is released in the atmosphere by volcanic activity and removed by forming carbonates. As the formation of carbonates is most efficient in the presence of liquid water, the surface temperature should not drop below 0°C for a long geological period. At high surface temperatures, the atmosphere is wet and thus water erosion and carbonate formation are enhanced. This scenario implies that CO₂ was the predominant greenhouse gas in the early atmospheres. Radiative-convective models [e.g. 16] suggest that only about 300 mbar CO₂ was required on early Earth to sustain the surface temperature above 0°C 4 Ga ago.

An implied warm climate on early Mars is more difficult to understand than on early Earth. On Mars, pressure levels of about 2 bars would be required for this, but at high CO₂ pressures, CO₂ condenses because of the low temperature in the middle atmosphere, forming high altitude ice clouds that strongly increase the albedo and thus decrease the surface temperature [17]. On the other hand, CO₂ ice clouds can be responsible for greenhouse warming due to the scattering of emitted infrared radiation from the surface, which may be stronger than the cooling effect due to the visible reflectivity of the clouds [18]. An efficient process known to limit CO₂ warming is Rayleigh back-scattering by air molecules in a dense atmosphere with pressure levels ≥ 5 bars, where the incoming visible radiation cannot reach the surface due to the scattering.

A recent study showed [19] that at high pressure a photochemically produced ozone layer may evolve on Mars, which can warm the middle atmosphere and

prevent the formation of CO₂ ice clouds. Taking into account the uncertainties in the collision-induced absorption (efficient at high pressures) of CO₂, even a 1 bar CO₂ atmosphere may have been enough to sustain 0°C at the Martian surface. High levels of CO₂ would have produced carbonates that have not been observed until now, neither on the oldest terrestrial rocks nor on Mars. On Earth, the missing carbonates would imply a CO₂ pressure lower than 10 mbar [20] 3 Ga ago, so an increase of the greenhouse effect by CH₄ was proposed, where the CH₄ production could have been related to biological activity. For the earliest stage of the Earth, before the emergence of life, it is not known if the temperature was maintained above 0°C by a high level of CO₂, abiotic CH₄ [21] or NH₃ [22] or if the Earth was globally frozen [23] at the exception of post-impact periods or local volcanic warming.

Another approach to a solution of these problems is the use of mass-losing solar models which are consistent with helio-seismology. Surface temperatures resulting in stable liquid water on Mars yield an initial mass between 1.03 to 1.07 times the present solar mass (M_{Sun}) [24]. Such considerations were recently supported by Hubble Space Telescope (HST) observations of HI Ly- α absorption lines from the region where stellar winds of young solar-like stars collide with the interstellar medium [25]. It was found that the mass loss rates of solar-like stars with the age of our Sun are of the same order and the loss rates of stars which arrived at ZAMS are 1000 times or more higher than at present. The cumulative mass loss rate obtained from these observations would yield a mass of the young Sun of about $1.03 \times M_{\text{Sun}}$ [25]. Such a slightly more massive young Sun together with a lower amount of greenhouse gases could have also been responsible for an early warm and wet Mars.

Problems in long-time stability of liquid water on the Martian surface are that such a massive young Sun would have lost most of its mass during the first hundred million years of its lifetime [22, 25]. The mass loss of the young Sun is directly related to a much denser early solar wind, which has important implications for the interaction with the Martian upper atmosphere after the planet's intrinsic magnetic field vanished.

Further, the time-dependence of the solar X-ray and extreme ultraviolet (EUV) flux I_{XUV} is critical for the evolution of thermal escape, ionisation, and photo-dissociation during the history of a planetary system. Estimates of the solar high-energy flux evolution are indirectly possible by the study of stellar proxies for the Sun at different ages. Multi-wavelength (from X-rays to the UV) observations have been collected for a sample of solar proxies within the *Sun in Time* program containing stars that represent most of the Sun's main sequence lifetime from 130 Ma to 7 Ga [26].

Observations obtained with the ASCA, ROSAT, EUVE, FUSE and IUE satellites cover a range between 1 and 3300 Å, except for a gap between 360 and 920 Å, which is a region of very strong interstellar medium absorption [26]. The resulting relative XUV fluxes yield an excellent correlation between the emitted flux and stellar age. In the relevant wavelength region of 1 to 1000 Å, the fluxes follow a power-law relationship $I_{\text{XUV}}(t)/I_{\text{XUV}} = 6.13 \times [t \text{ (Ga)}]^{-1.19}$.

Table 2.1 XUV flux normalised to the present value as a function of time after the Sun arrived at ZAMS.

Age [Ga]	0.1	0.3	0.5	1	1.5	2	2.5	3	3.5	4	4.5
$I_{\text{XUV}}(t)/I_{\text{XUV}}$	95	25.7	14	6.13	3.78	2.68	2.07	1.66	1.38	1.17	1

The relationship shown in Table 2.1 indicates XUV fluxes of about $6 \times I_{\text{XUV}}$ about 3.5 Ga ago, and about $100 \times I_{\text{XUV}}$ about 100 Ma after the Sun's arrival at ZAMS. Thus, these high XUV fluxes of the young Sun heated the early upper Martian atmosphere and were responsible for large thermal escape rates of water-based photo-dissociated hydrogen as well as for efficient photo-ionisation and photo-dissociation reactions of atmospheric constituents like CH_4 or NH_3 , which are important for greenhouse effects.

2.1.3 XUV-Driven Hydrodynamic Escape

Recent modelling of atmospheric evolution on terrestrial planets has focused on fractionation from primordial source compositions during XUV-driven hydrodynamic escape [e.g. 27]. The upper atmospheres of terrestrial planets are mainly controlled by absorption of XUV radiation [28] and additionally by energy deposited in the upper atmospheres by large impacts [29]. By knowing the evolution of the solar XUV radiation with time, one can apply a scaling relation for the estimation of the exosphere temperature (T_∞) responsible for thermal escape over the Martian history. This relation is based on the assumption of equilibrium between XUV heat input and downward heat transport by conduction.

Below the exosphere (in the thermosphere), the effective heat production is balanced by the divergence of a conductive heat flux of the XUV radiation leading (after some approximations) to $T_\infty^* \approx [(\varepsilon I_{\text{XUV}} k \sigma_c) / (k_0 m g \sigma_a)] + T_0^*$, where ε is the heating efficiency, σ_c and σ_a are the collision and absorption cross sections, respectively, k is the Boltzmann constant, s depends on the thermospheric composition in the thermal conductivity coefficient $K(T) = K_0 T^s$, m is the mass of the main thermospheric constituent, g is the acceleration of gravity and T_0 is the mesopause temperature. By knowing the planetary parameters at present time t_1 one can estimate T_∞ in the Martian past t_0 from the scaling relation $(T_\infty^* - T_0^*)_1 / (T_\infty^* - T_0^*)_0 \approx I_{\text{XUV}1} g_0 / I_{\text{XUV}0} g_1$ [30].

When T_∞ is large and the thermal escape parameter $X = GMm/kT_\infty r$ (where G is the gravitational constant, M is the planetary mass and r is the planetary distance) reaches values ≤ 1.5 , the exosphere becomes unstable and hydrostatic equilibrium no longer applies [31].

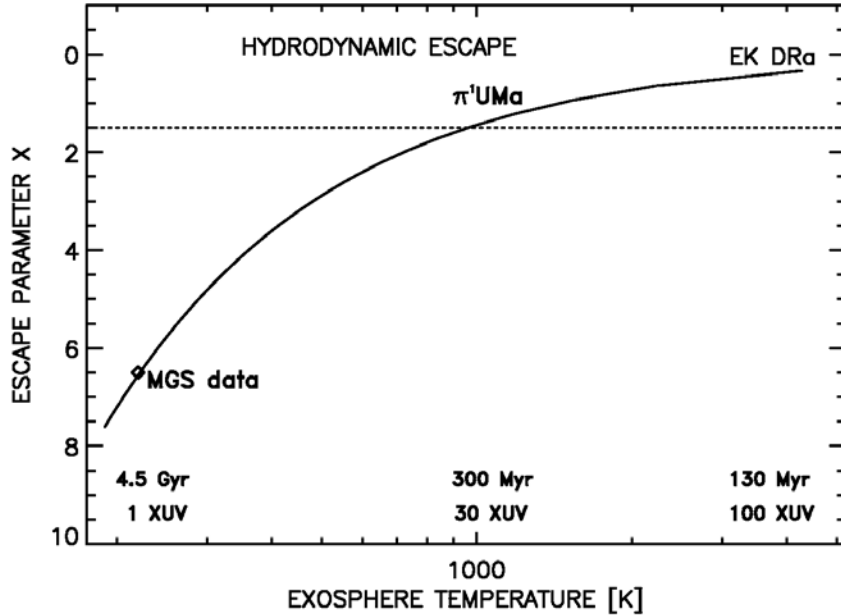


Fig. 2.1. Escape parameter X for H atoms on Mars as a function of exosphere temperature T_∞ and XUV flux at an orbital distance of 1.5 AU and time. The dotted line marks the area where hydrodynamic escape becomes important since $X \leq 1.5$. MGS corresponds to the present exosphere temperature observed by Mars Global Surveyor. One can see that an early Martian CO_2 atmosphere was probably affected by hydrodynamic escape for hydrogen during the first 300 Ma (age of solar proxy π^1 UMa) after the origin of the planet. The efficient loss of hydrogen during this period may have removed the majority of the initial Martian water by diffusion-limited escape and could have been responsible for the enrichment of D isotopes close to the cometary D/H ratio as found in Martian Shergottite meteorites.

By considering the hydrodynamic treatment it is found that for Mars $T_\infty \geq 1000$ K, the thermal energy becomes comparable to the gravitational potential energy ($3kT_\infty > 2MmGr$) and the light atmospheric constituents like hydrogen flow away, limited only by the incoming XUV flux and by the diffusion through the heavy major atmospheric constituent CO_2 [e.g. 27]. One can see from Fig. 2.1 that Mars experienced diffusion-limited hydrodynamic escape of hydrogen from its primordial water inventory at least during the first 300 Ma after the planetary formation. Studies on diffusion-limited hydrodynamic loss due to the young Sun predict escape rates of hydrogen in the order of about 10^{28} to 10^{29} s^{-1} from Mars [8, 27, 32]. These escape rates are large enough to remove the amount of hydrogen from an equivalent terrestrial ocean in about 300 Ma.

Under such extreme conditions, the hydrogen escape fluxes are large enough to exert upward drag forces on heavier atmospheric constituents sufficient to lift them out of the atmosphere. Lighter species are entrained with the out-flowing

hydrogen and lost more readily than heavier ones, leading to mass fractionation of the residual atmosphere.

2.1.4 Impact Erosion

Over the last few decades, it has become clear that impacts of asteroids, comets and other Solar System bodies played a fundamental role in the evolution of terrestrial planets and their atmospheres. As discussed in Section 2.1.1, impacts are a primary mechanism of planetary accretion and are responsible for the delivery of water and organic matter to young planetary bodies. Large impactors may have also inhibited the formation of life in the early history of planetary formation.

Thus, the impact of a planetesimal can erode part of an existing atmosphere or it can add volatiles to it. The balance on delivery and loss from an atmosphere depends on the composition of the impactor and on the mass of the growing planet [27, 33]. When Venus and Earth attained their present masses and escape velocities, impact erosion became very inefficient, but Mars with its smaller mass was rather vulnerable and still would it be if the impact population had not essentially died out. Impact studies on Mars show that the planet could have lost a CO₂ atmosphere between 5 and 10 bars due to impact erosion over the first Ga [33]. Once an atmosphere had been eroded, it could have been resublimed by comets [34].

There is also evidence that the Martian water after the end of the heavy bombardment may have been enriched with cometary sources, after the majority of the initial water was lost by diffusion-limited hydrodynamic escape, because the average value of about 2.3 times the TSW ratio measured in the Shergottites [12, 35, Chap. 1 by Baker et al.] fits well the observed D/H ratio in comets Halley [36], Hyakutake [37] and Hale-Bopp [38]. These rates are all about twice the value for terrestrial seawater, but are consistent with rates in “hot cores” of molecular clouds. It is believed that ion-molecule reactions in dense molecular clouds at temperatures close to 35 K can produce these D/H enrichments.

2.1.5 The Early Martian Magnetic Field

Intrinsic planetary magnetic fields are responsible for the protection of atmospheres against the solar wind. The available data of an early Martian magnetic field are restricted to measurements by Mars Global Surveyor (MGS) and the study of Martian meteorites [e.g. 39]. In 1997, MGS started with the global mapping of the Martian magnetic environment and found that the planet does not have a significant global intrinsic magnetic field [40]. However, these measurements also established the presence of significant, local, small-scale, crustal, remnant magnetisation.

This local magnetisation appears mainly in the ancient southern highlands, and is absent in the regions where large impacts occurred (like Hellas and Argyre).

Since these impact basins were formed about 4 Ga ago, it is generally argued that the Martian dynamo ceased before this time [41]. Another study used the same data and suggested that the Martian dynamo turned on less than 4 Ga ago, and turned off at an unknown time since then, with the only limitation that the present magnetic field strength must be achieved [42].

Magnetic studies of the Martian meteorite ALH 84001 revealed that about 4 Ga old carbonates contained magnetite and pyrrhotite, which carried a stable natural remnant magnetisation [43]. This result implies that Mars had established a geodynamo within 450 to 650 Ma after its formation with an intensity within an order of magnitude of that of the present Earth. Moreover, these results support the theory that an ancient strong dynamo ceased about 4 Ga ago. The remnant magnetism of Martian SNC meteorites, which formed 1.3 Ga to 180 Ma ago, is consistent with both theories since such field strengths could appear at the surface of Mars even at present [44].

The assumed/indicated intrinsic magnetic field, which is comparable to the terrestrial one, should have protected the atmosphere from the dense solar wind of the young Sun. On the other hand, these studies indicate that the Martian atmosphere may have been unprotected and affected by various non-thermal escape processes by the solar wind plasma during the past 3.5 Ga.

2.2 Thermal Atmospheric Escape (Jeans Escape)

Light molecules in the exosphere can be thermally driven to escape (Jeans escape) when the velocity exceeds the escape velocity.

The order of the thermal escape flux of hydrogen atoms from present Mars can be estimated, by assuming an exosphere temperature which fits H Ly- α day glow observations, to be about $1.8 \times 10^8 \text{ cm}^{-2} \text{ s}^{-1}$ ($1.5 \times 10^{26} \text{ s}^{-1}$) [45]. Recent observations of four H₂ lines in a spectrum of Mars with the FUSE satellite revealed a column abundance of molecular hydrogen of $1.17 \times 10^{13} \text{ cm}^{-2}$, 140 km above the Martian surface, resulting in an H₂ mixing ratio of 15 ± 5 parts per million in the lower Martian atmosphere [46]. By using this value, one gets a thermal H₂ escape flux of about $4 \times 10^6 \text{ cm}^{-2} \text{ s}^{-1}$ ($3.3 \times 10^{24} \text{ s}^{-1}$). One can see that the thermal H₂ loss rate is thus negligibly small when compared to the atomic H loss rate. Therefore, one derives a total thermal escape flux of present hydrogen atoms of about $1.8 \times 10^8 \text{ cm}^{-2} \text{ s}^{-1}$ ($1.5 \times 10^{26} \text{ s}^{-1}$). However, significant progress in the determination of uncertainties of the Martian exosphere temperature and related hydrogen loss rates is expected from Mars Express in 2004 and 2005.

2.3 Non-Thermal Atmospheric Escape

2.3.1 Ion Pick Up

Neutral gas particles can get ionised above the Martian ionopause and picked up by the solar wind. Measurements by the ASPERA (Automatic Space Plasma Experiment with a Rotating Analyser) instrument aboard the Phobos 2 spacecraft have shown that the plasma tail of Mars consists mainly of ions coming from the Martian atmosphere [e.g. 47]. For studying the O^+ ion pick up escape rates from Mars we used a test particle model that involves the motion in the environmental electric and magnetic fields based on the *Spreiter-Stahara* model [e.g. 48, 49] and obtained for average solar activity conditions a total pick up escape flux for hydrogen ions of about $3 \times 10^6 \text{ cm}^{-2} \text{ s}^{-1}$ ($3.0 \times 10^{24} \text{ s}^{-1}$).

For the calculation of past pick up ion escape rates and pick up ion sputtering, one must be able to estimate the hot oxygen corona density in the Martian past. One can use the National Center for Atmospheric Research (NCAR) non-LTE (local thermal equilibrium) one-dimensional code as a modelling tool for the estimation of the average properties of the ancient Martian thermosphere and ionosphere for the calculation of the hot particle coronae [50]. By deducing the corona profiles from the results of the code mentioned above, one can study the role of molecular species in pick up ion sputtering of the ancient Martian atmosphere [51, 52].

By using similar density profiles for the average pick up O^+ ion loss estimations of about $4.5 \times 10^7 \text{ cm}^{-2} \text{ s}^{-1}$ ($3.8 \times 10^{25} \text{ s}^{-1}$) and about $9.6 \times 10^8 \text{ cm}^{-2} \text{ s}^{-1}$ ($8 \times 10^{26} \text{ s}^{-1}$) for the 2 Ga and 3.5 Ga periods, we note that O^+ ion pick up loss rates in a previous study [50] are about 10 times and 2 times larger, respectively, than those found in our calculations. The main reason for these discrepancies is their use of different solar wind density values for the 2 Ga and 3.5 Ga epochs, for which we used the observation-based stellar wind data [22] as discussed above.

2.3.2 Detached Ionospheric Clouds Triggered by Magnetohydrodynamic Instabilities

Another atmospheric loss process on Mars is the occurrence of magnetohydrodynamic (MHD) instabilities at the boundary layer between the solar wind and the atmospheric plasma [53, 54]. Since there is a shear velocity between the plasma flow in the solar wind (magnetosheath) and the plasma in the ionosphere, the so called Kelvin-Helmholtz (KH) instability can develop and evolve into a nonlinear stage, where ionised atmospheric constituents can detach from the ionosphere in the form of plasma clouds [55].

It was found by the Pioneer Venus Orbiter (PVO) that plasma clouds are a common feature caused by the solar wind-ionosphere interaction on Venus [56]. Analysis of data by the MAG/ER (Magnetometer/Electron Reflectometer) instru-

ment of MGS revealed cold electrons above the Martian ionopause, which indicate the presence of plasma clouds also on Mars [40].

It is found that near the Martian subsolar point the velocity shear is very small, indicating that this region is stable against the KHz-instability [57]. But near the terminator, the KHz-instability can occur since the velocity shear is much larger there. The highest velocity in the magnetosheath appears at the flanks near the terminator plane due to the Lorentz force accelerating the plasma. Therefore, we assume that the KHz-instability appears also in this region.

A statistical analysis of the situation on Venus [56] scaled to Martian conditions for the estimation of O^+ ion escape shows that this process can contribute to present escape fluxes between $1.2 \times 10^5 \text{ cm}^{-2} \text{ s}^{-1}$ and $6 \times 10^6 \text{ cm}^{-2} \text{ s}^{-1}$ (10^{23} s^{-1} and $5 \times 10^{24} \text{ s}^{-1}$). Due to the higher solar wind mass flux and ionospheric densities in the past [51] we estimate O^+ ion escape fluxes of about $9.5 \times 10^6 \text{ cm}^{-2} \text{ s}^{-1}$ ($8 \times 10^{24} \text{ s}^{-1}$) 2 Ga ago and about $2.3 \times 10^8 \text{ cm}^{-2} \text{ s}^{-1}$ ($2 \times 10^{26} \text{ s}^{-1}$) 3.5 Ga ago.

2.3.3 Ion Loss due to Momentum Transport Effects

The outflow of cold ionospheric ions from the Martian terminator regions was also observed by the ASPERA instrument on board of the Phobos 2 spacecraft, which indicates a strong interaction between the solar wind plasma and the cold ionospheric plasma in the Martian topside ionosphere in a way that the solar wind plasma transfers momentum directly to the ionosphere in a dayside transition region to the deep plasma tail [47]. PVO measured on Venus the median velocity field of O^+ ions on the outbound portion of orbits from periaapsis to the ionopause and found that the bulk velocity of the ions near the terminator is about 5 km s^{-1} [58], which is the escape velocity of O atoms on Mars.

The results of several studies [58, 59, 60] suggest that the solar wind momentum transport seems to be capable of accelerating ionospheric O^+ ions to velocities $\geq 5 \text{ km s}^{-1}$ ($\geq 2 \text{ eV}$) resulting in energies larger than the Martian escape energy. In a previous study [58], it was shown that cool ion escape due to momentum transport effects may have removed water from Mars equivalent to a global ocean with a thickness of about 10 to 30 m, depending on the uncertainties of solar wind parameters and the Martian plasma environment in the past.

We studied this loss process by using the observed average stellar wind data of young solar-like stars [22, 52] and the ionospheric density profiles corresponding to the Martian history [50] and found an additional escape rate of oxygen of about $1 \times 10^{25} \text{ s}^{-1}$ at present, about $2 \times 10^{26} \text{ s}^{-1}$ 2 Ga ago and about $2 \times 10^{27} \text{ s}^{-1}$ 3.5 Ga ago. One can see that this loss process may have played an important role in the Martian history because it is strongly related to the solar wind and ionospheric density, which was much larger due to the more active young Sun.

2.3.4 Atmospheric Sputtering

Particles which hit the Martian atmosphere are responsible for sputtering loss of neutral constituents. Loss rates for O atoms and CO₂ molecules on Mars were studied in the past [52 and references given therein] and yielded escape flux values of about $3.6 \times 10^5 \text{ cm}^{-2} \text{ s}^{-1}$ ($3 \times 10^{23} \text{ s}^{-1}$) both for O atoms and for CO₂ molecules. A 1-D Monte Carlo type atmospheric sputtering model, which considered anisotropic scattering functions and energy-dependent cross sections, resulted in sputtering fluxes for O and CO₂ of about $5.6 \times 10^6 \text{ cm}^{-2} \text{ s}^{-1}$ ($4.7 \times 10^{24} \text{ s}^{-1}$) and $2.9 \times 10^6 \text{ cm}^{-2} \text{ s}^{-1}$ ($2.4 \times 10^{24} \text{ s}^{-1}$), respectively [e.g. 61]. In a recent study, the sputtered population inside the hot corona was modelled and the escaping particles were studied by using a sophisticated 3-D test particle model, whereas the heating effect due to the incident particle flux was described by using a 2-D direct Monte Carlo simulation [51].

The results of such a sophisticated model yield a present Martian average sputtering escape flux of O atoms of about $7 \times 10^5 \text{ cm}^{-2} \text{ s}^{-1}$ ($6.5 \times 10^{23} \text{ s}^{-1}$) and indicate that the standard 1-D models overestimate the sputtering yield by about 15 – 25 % when corrected for coronal ejection. Further, by coupling a test particle Monte Carlo approach with a molecular dynamic model to describe the collisions between hot particles and cold molecules in the Martian atmosphere, one finds total present sputtering escape fluxes for O atoms of about $5.2 \times 10^5 \text{ cm}^{-2} \text{ s}^{-1}$ ($4.3 \times 10^{23} \text{ s}^{-1}$) [52]. By using this 3-D model, an O escape flux for sputtering of about $1.5 \times 10^8 \text{ cm}^{-2} \text{ s}^{-1}$ ($1.3 \times 10^{26} \text{ s}^{-1}$) 2 Ga ago and of about $1.8 \times 10^9 \text{ cm}^{-2} \text{ s}^{-1}$ ($1.5 \times 10^{27} \text{ s}^{-1}$) 3.5 Ga ago is found.

2.3.5 Dissociative Recombination

Dissociative recombination of ionospheric O₂⁺ ions produces very low energetic neutral O atoms, where a fraction can escape and the other part can form a planetary corona. Based on the first measurements obtained by Mariner 4, an average escape flux into space of hot O atoms produced via this process on the dayside hemisphere is about $6 \times 10^7 \text{ cm}^{-2} \text{ s}^{-1}$ ($5.0 \times 10^{25} \text{ s}^{-1}$) and was estimated by the simplified assumption that atoms are emitted with equal probability in the upward and downward directions [62].

Monte Carlo models that followed the hot O atoms by including collisions and energy loss on their way up to the exosphere [52 and references given therein] found a reduction in the average escape flux of hot O atoms by about one order of magnitude, i.e. $6 \times 10^6 \text{ cm}^{-2} \text{ s}^{-1}$ ($5 \times 10^{24} \text{ s}^{-1}$). The observational results for the evolution of the solar XUV flux with time obtained by solar proxies agree well with the values used by [50]. Thus, the exospheric O escape fluxes of about $3.6 \times 10^7 \text{ cm}^{-2} \text{ s}^{-1}$ ($3 \times 10^{25} \text{ s}^{-1}$) 2 Ga ago and about $9.7 \times 10^7 \text{ cm}^{-2} \text{ s}^{-1}$ ($8 \times 10^{25} \text{ s}^{-1}$) 3.5 Ga ago may be accurate and should represent realistic values [50, 63].

2.3.6 Oxygen Loss into the Martian Soil

Our escape studies show that the H:O escape ratio of 2:1 assumed by some equilibrium photo-chemical atmospheric models requiring a steady state [64] cannot be maintained due to the heavier mass of O. Since oxygen can react with the surface, the ratio can be obtained. We estimate that about 10^{42} oxygen particles have been incorporated into the Martian soil since about 2 Ga ago. Ferric oxides and sulphates are the most important candidate phases in regard to oxidation products. In the light that Martian precursor mineralogy, introduced by meteoritic infall [65] and indigenous rocks, comprises such polyvalent elements as iron and sulphur in considerable lower oxidation states than present in ferric oxides and sulphates, this is an important sink of atmospheric oxygen [52 and references given therein].

Based on the meteoritic contribution to the Martian surface [66] typical soils analysed by Mars Pathfinder appear to contain three components: lithic fragments, meteoritic matter and physical fractionation products of parent andesites with typical initial oxidation states. Analyses of ferric absorption edges in reflectance spectra of Alpha Proton X-Ray Spectrometer (APXS) spots give hints to absolute oxidation states of the soil if combined with variation in the chemical space. Assuming correspondingly initial $\text{Fe}^{3+}/\text{Fe}^{\text{tot}}$ ratios of 0.4 and final ones of 0.6 this would lead to global soil horizons between 4 to 15 metres. Using models of meteoritic gardening [67, 68, 69], this would yield regolith depths between 7 and 150 metres resulting in corresponding oxidant extinction depths between 2 and 5 metres. These results span a range of extreme values depending on sulphate formation from emanation of sulphuric volcanic gases or from oxidation of magmatic sulphides [52]. However, the modelling of oxidant extinction depths and meteoritic gardening given in [67] are based on oxidant diffusion into the soil column. If oxidation processes occur outside of the soil, e.g. during atmospheric entry of cosmic matter [66] or in the context of heat input above the threshold for thermal oxidation associated with impact processes [70], the oxidant extinction depths would be significantly reduced.

Further, the strong atmosphere-surface interaction between oxygen and the Martian soil may produce adsorbed superoxides (O_2^-). Such species were observed on Martian analogue materials upon UV-illumination by means of experiments under simulated Martian environmental conditions [71]. Although the formation processes and diffusive capabilities of superoxides and related oxidants are far from being resolved [72], it seems to be evident that *in situ* oxidation on the Martian surface is an active process. Photo-oxidation experiments on magnetite as the precursor material found that such a process should be involved in active and efficient oxidation on the Martian surface [73]. That the Martian surface is oxidizing not only at the top surface due to UV-radiation but also in the subsurface was confirmed by the negative response of Viking biology experiments and the evidence for reversibly bound oxygen bearing agents as an outcome of Viking gas exchange experiments on subsurface soil samples [74, 75].

2.3.7 Total Water Loss Since 3.5 Ga

Table 2.2 Summary of oxygen-related atmospheric constituents lost from Mars over the past 3.5 Ga. Given are the number of molecules or atoms.

Age [Ga]	Present [s^{-1}]	2 Ga ago [s^{-1}]	3.5 Ga ago [s^{-1}]
PU: O^+	3×10^{24}	3.8×10^{25}	8×10^{26}
DR: O	2.8×10^{24}	3×10^{25}	8×10^{25}
SP: O	2.2×10^{23}	7×10^{25}	1.3×10^{27}
SP: CO	3.5×10^{22}	2.3×10^{24}	4×10^{25}
SP: CO_2	5×10^{22}	2×10^{24}	2.5×10^{25}
PC: O^+	1×10^{24}	8×10^{24}	2×10^{26}
MT: O^+	1×10^{25}	2×10^{26}	2×10^{27}
Total O loss	1.7×10^{25}	6.5×10^{26}	5.4×10^{27}

The maximum total loss of oxygen-related constituents from Mars (Table 2.2) caused by ion pick up (PU), dissociative recombination (DR), sputtering (SP), plasma clouds (PC) and momentum transport (MT) over the past 3.5 Ga was estimated to be equivalent to a global Martian water ocean with a layer thickness of about 35 m by using oxygen as an upper limit for the water loss [76] as assumed by equilibrium photochemical atmospheric models, which require a steady state between the H:O escape ratio of 2:1 [64]. However, by assuming that the hydrogen escape flux represents an upper limit for an equivalent water loss to space one obtains a lower value of 5 m [79, 80, 81]. If this assumption is true and the stoichiometrically desirable ratio 2:1 of H and O escape was not maintained before 2 Ga ago, the majority of oxygen lost to space would have to have originated from CO_2 instead of H_2O . One can see from Table 2.2 that the 2:1 ratio between the H:O loss to space is not established at present. The present uncertainties in the estimation for the atmospheric escape rates caused by plasma instabilities and momentum transport processes will be minimised after the analysis of Mars Express' ASPERA-3 data.

2.4 Evolution of the Martian Water Inventory

The D isotopes in the Martian atmosphere have been detected by the resolution of several Doppler-shifted lines of HDO vapour near 3.7 micrometre in the planetary spectrum, which revealed an enrichment compared to the D/H ratio of the TSW value by a factor 5 [7, 8]. Given the large size of water reservoirs on Earth, one can assume that the D/H ratio has not changed much in the terrestrial seawater during the past billion years.

As discussed before, the initial D/H ratio in Martian water reservoir originates from impacts of asteroids and comets and may have been in the order of about 1.2

to 1.6 times the TSW ratio [9]. Measurements in Martian SNC meteorites also yield D/H ratios of about 1 to 2.3 times the TSW value [35, 76]. The measured D/H ratio of the 3.9 Ga old ALH 84001 meteorite is about 1.6 times the TSW. The simplest interpretation of the D enrichment in the Martian atmosphere is that an appreciable amount of H associated with the original water or water-ice reservoir escaped to space.

By knowing the fractionation factor f between D and H and the initial isotope ratio one can estimate the value $r(t) = [R(t)/R(t_0)]^{1/(1-f)}$, which indicates how many times the water-ice reservoir, which is in isotopic exchange with the present Martian atmosphere, was larger in the past. Observations with the Goddard High-Resolution Spectrograph at the HST indicate that f lies between 0.016 and 0.02 in the lower Martian atmosphere [76]. R is the isotope ratio between D and H at two different times t_0 (earlier) and t_1 .

By using f of about 0.016, one finds that the Martian water-ice reservoir was about 5.26 times larger if the initial isotope ratio was the TSW value and about 4.36 times larger for 1.2 times the TSW, 3.26 times larger for 1.6 times the TSW, and 2.25 times larger for 2.3 times the TSW, respectively. By knowing the total amount of water $L_{\text{H}_2\text{O}}$ (equivalent depth) lost over the Martian history, one obtains a constraint on the thickness $s(t) = L_{\text{H}_2\text{O}}/[r(t)-1]$ in terms of an equivalent depth [e.g. 8, 76]. Figure 2.2 shows the present water-ice reservoir, which is in isotopic exchange with the Martian atmosphere, as a function of the equivalent depth $L_{\text{H}_2\text{O}}$ lost from the planet over 3.5 Ga. Since the Martian obliquity oscillates on time scales of about 10^5 to 10^7 years between 0° and 60° , one can expect dramatic climate changes and effective isotope exchange between the ice deposits and the atmosphere [77].

The solid line in Fig. 2.2 corresponds to the TSW ratio, the dashed-dotted line to a D enrichment of 1.2 times the TSW ratio, the dashed line to a D enrichment of 1.6 times the TSW ratio [9], and the dashed-dotted-dotted line to a D enrichment of about 2.3 times the corresponding TSW ratio as measured in Martian SNC meteorites and comets [35], respectively. One can see from the estimates in Fig. 2.2 that Mars should presently possess a water-ice reservoir which can interact with the atmosphere with an equivalent depth of a few m up to 27 m, depending on initial isotope D/H ratios and water loss rates.

By using the values obtained for $r(t)$ we find a water-ice reservoir exchangeable with the Martian atmosphere 3.5 Ga ago with an equivalent depth of about 15 to 60 m, depending on the initial D/H ratios assumed.

From MOLA data an ice volume can be estimated, which corresponds to an equivalent depth of about 9 m [13]. One can see from Fig. 2.2 that this value agrees with our estimation if the initial D/H ratio was close to the TSW value or 1.2 times the TSW ratio and an equivalent global water layer with a depth of about 34 m was lost to space. On the other hand, if the initial D/H isotope ratio was 1.6 times the TSW ratio, an equivalent depth of about 15 m should have been lost to space over 3.5 Ga. If the initial D/H ratio was about 2.3 times the TSW value, the lower escape value would yield an equivalent depth of about 11 m, while the upper escape rate would yield about 27 m [76].

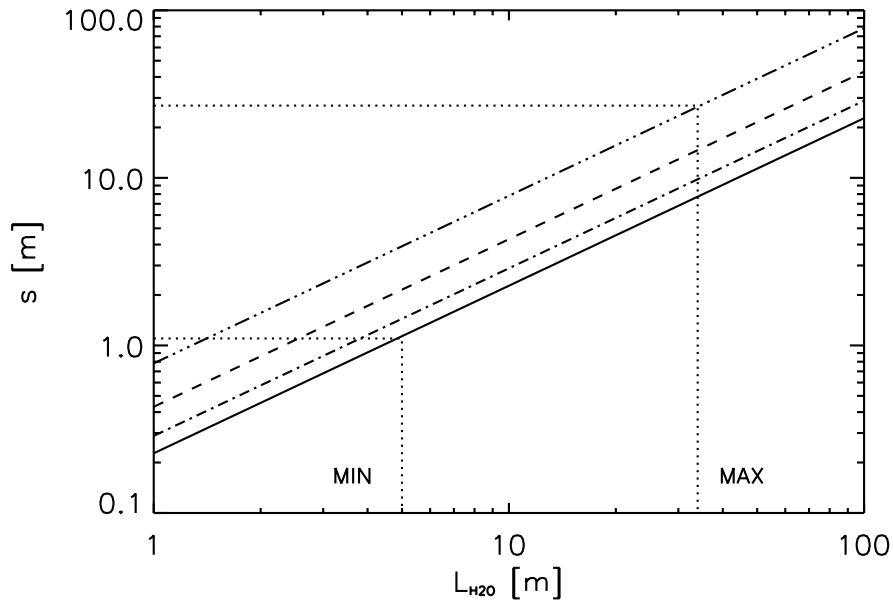


Fig. 2.2 Estimated minimum (MIN) and maximum (MAX) present Martian surface water-ice reservoir in terms of the equivalent depth s (dotted lines), which is in isotopic exchange with the atmosphere, as a function of total water lost $L_{\text{H}_2\text{O}}$ from Mars over the past 3.5 Ga with various initial D/H isotope ratios. The solid line has an initial D/H ratio equal to the TSW value. The dashed-dotted and dashed lines have D/H ratios of 1.2 times and 1.6 times the TSW value [9], respectively, and the dashed-dotted-dotted line correspond to the average D/H value measured in Martian Shergottite meteorites of about 2.3 times the TSW value which is comparable to the D/H ratio in comets [35].

Although there are uncertainties, our estimation shows that the water-ice reservoir which is in isotopic exchange with the atmosphere can be lower but also three times the estimated water-ice available in the Martian northern polar cap. By using the estimated water reservoirs 3.5 Ga ago related to the 2.3 times the TSW value we can estimate the minimum and maximum reservoirs, where the D/H isotope ratio was enriched from 1.2 or 1.6 times the TSW value due to hydrodynamic escape. One gets water reservoirs affected by isotopic fractionation with an equivalent depth of between 35 and 115 m, depending on the initial isotope ratios in Martian water 4.5 Ga ago.

2.5 Conclusions

Our study obtained from atmospheric evolution shows that Mars may presently contain a subsurface water-ice reservoir which can exchange with the atmosphere with an equivalent depth of a few metres to 27 m. Much better estimations of the

present and past Martian water-ice reservoirs in isotopic exchange with the atmosphere over the planetary history will probably be possible after exact ion and neutron particle outflow measurements by the ASPERA-3 instrument on board the Mars Express. These observations will reduce the uncertainties in the current estimations of atmospheric loss caused by solar wind plasma interactions with the ionospheric environment. If the Martian subsurface also hides a bulk water-ice reservoir which is not exchangeable with the atmosphere and is a remainder of the initial water source, it could only be determined by radar sounding such as by the MARSIS instrument on board of Mars Express. Should MARSIS not detect such an additional reservoir, this would mean that such a reservoir may have been lost due to hydrodynamic escape and impact erosion before 3.5 Ga ago.

Further, by assuming that all hydrogen lost to space originates from water, our study suggests that the stoichiometrically desirable H:O escape ratio of 2:1 to space could not be maintained since about 2 Ga ago. This result implies an oxygen surface sink and a strong atmosphere-surface interaction, which may be responsible for an enhanced soil/surface oxidation process. It is possible to incorporate this amount of oxygen into the regolith by oxidation of inorganic soil-precursors. Depending on different models of meteoritic gardening, the expected range for the oxidant extinction depth should be between 2 and 5 m. These constraints on the oxidant extinction depth are important for the search of organic material since *in situ* excavation of samples from the subsurface with penetrating moles or drilling equipment.

Acknowledgements

I. Ribas acknowledges support from NASA FUSE grants NAG5-8985, NAG5-10387 and NAG5-12125.

2.6 References

- 1 Pepin RO (1994) Evolution of the Martian Atmosphere. *Icarus* 111: 289-304
- 2 Hutchins KS, Jakosky BM (1996) Evolution of Martian atmospheric argon: implications for sources of volatiles. *J. Geophys. Res.* 101 (E6): 14933-14949
- 3 Carr MH (1999) Retention of an atmosphere on early Mars. *J. Geophys. Res.* 104 (E9): 21897-21909
- 4 Morbidelli A, Chambers J, Lunine JJ, Petit JM, Robert F, Valsecchi GB, Cyr KE (2000) Source regions and timescales for the origin of water on Earth. *Meteorit. Planet. Sci.* 35: 1309-1320
- 5 Robert F (2001) The origin of water on Earth. *Science* 293: 1056-1058
- 6 Petit J-M, Morbidelli A, Chambers J (2001) The primordial excitation and clearing of the asteroid belt. *Icarus* 153: 338-347
- 7 Owen TC (1992) The composition and early history of the atmosphere of Mars. In: Kieffer HH, Jakosky BM, Snyder CW, Matthews MS (eds) *Mars*. University of Arizona Press, Tucson, pp. 818-834
- 8 Donahue TM (1995) Evolution of water reservoirs on Mars from D/H ratios in the atmosphere and crust. *Nature* 374: 432-434

- 9 Lunine JI, Chambers J, Morbidelli A, Leshin LA (2003) The origin of water on Mars. *Icarus* 165: 1-8
- 10 Carr MH (1996) *Water on Mars*. Oxford University, New York
- 11 Baker VR (2001) Water and the Martian landscape. *Nature* 412: 228-236
- 12 Leshin LA (2000) Insights into Martian water reservoirs from analysis of Martian meteorite QUE94201. *Geophys. Res. Lett.* 27: 2017-2020
- 13 Zuber MT, Smith DE, Solomon SC, Abshire JB, Afzal RS, Aharonson O, Fishbaugh K, Ford PG, Frey HV, Garvin JB, Head III JW, Ivanov AB, Johnson CL, Muhleman DO, Neumann GA, Pettengill GH, Phillips RJ, Sun X, Zwally HJ, Banerdt WB, Duxbury TC (1998) Observations of the north polar region of Mars from the Mars Orbiter Laser Altimeter. *Science* 282: 2053-2060
- 14 Sagan C, Mullen G (1972) Earth and Mars: evolution of atmospheres and surface temperatures. *Science* 177: 52-56
- 15 Walker JCG, Hays PB, Kasting JF (1981) A negative feedback mechanism for the long-term stabilization of Earth's surface temperature. *J. Geophys. Res.* 86: 9776-9782
- 16 Kasting J (1988) Runaway and moist greenhouse atmospheres and the evolution of Earth and Venus. *Icarus* 74: 472-494
- 17 Kasting J (1991) CO₂ condensation and the climate of early Mars. *Icarus* 94: 1-13
- 18 Forget F, Pierrehumbert RT (1997) Warming early Mars with carbon dioxide clouds that scatter infrared radiation. *Science* 278: 1273-1276
- 19 Selsis F, Despois D, Parisot J-P (2002) Signature of life on exoplanets: can Darwin produce false positive detections? *Astron. Astrophys.* 388: 985-1003
- 20 Rye R, Kuo PH, Holland HD (1995) Atmospheric carbon-dioxide concentrations before 2.2-billion years ago. *Nature* 378: 603-605
- 21 Pavlov AA, Kasting JF, Brown LL, Rages KA, Freedman R (2000) Greenhouse warming by CH₄ in the atmosphere of early Earth. *J. Geophys. Res.* 105(E5): 11981-11990
- 22 Sagan C, Chyba C (1997) The early faint Sun paradox: organic shielding of ultraviolet-labile greenhouse gases. *Science* 276: 1217-1221
- 23 Sleep NH, Zahnle, K (2001) Carbon cycling and implications for climate on ancient Earth. *J. Geophys. Res.* 106(E1): 1373-1400
- 24 Sackmann I-J, Boothroyd AI (2003) Our Sun. V. A bright young Sun consistent with helioseismology and warm temperatures on ancient Earth and Mars. *Astrophys. J.* 583: 1024-1039
- 25 Wood BE, Müller H-R, Zank G, Linsky JL (2002) Measured mass loss rates of solar-like stars as a function of age and activity. *Astrophys. J.* 574: 412-425
- 26 Guinan EF, Ribas I (2002) Our changing Sun: the role of solar nuclear evolution and magnetic activity on Earth's atmosphere and climate. In: Montesinos B, Giménez A, Guinan EF (eds) *The Evolving Sun and its Influence on Planetary Environments*, ASP Conference Proc. 269: 85-107
- 27 Hunten DM, (1993) Atmospheric evolution of the terrestrial planets. *Science* 259: 915-920
- 28 Bauer SJ (1971) Solar cycle variation of planetary exospheric temperatures. *Nature* 232: 101-102
- 29 Pepin RO (1997) Evolution of Earth's noble gases: consequences of assuming hydrodynamic loss driven by giant impact. *Icarus* 126: 148-156
- 30 Bauer SJ, Hantsch MH (1989) Solar cycle variation of the upper atmosphere temperature of Mars. *Geophys. Res. Lett.* 16: 373-376
- 31 Öpik EJ (1963) Selective escape of gases. *Geophys. J. Roy. Astron. Soc.* 7: 490-509
- 32 Kasting JF, Pollack JB (1983) Loss of water from Venus I. Hydrodynamic escape of hydrogen. *Icarus* 53: 479-508
- 33 Melosh HJ, Vickery A (1989) Impact erosion of the primordial atmosphere of Mars. *Nature* 338: 487-489

- 34 Owen T, Bar-Nun A, Kleinfeld I (1992) Possible cometary origin of noble gases in the atmospheres of Venus, Earth and Mars. *Nature* 358: 43-46.
- 35 Leshin LA, Epstein S, Stolper EM (1996) Hydrogen isotope geochemistry of SNC meteorites. *Geochim. Cosmochim. Acta* 60: 2635-2650
- 36 Eberhardt P, Reber M, Krankowsky D, Hodges RR (1995) The D/H and $^{18}\text{O}/^{16}\text{O}$ ratios in water from comet P/Halley. *Astron. Astrophys.* 302: 301-316
- 37 Bockelée-Morvan D, Gautier D, Lis DC, Young K, Keene J, Phillips T, Owen TC, Crovisier J, Goldsmith PF, Bergin EA, Despois D, Wooten A (1998) Deuterated water in comet C/1996 B2 (Hyakutake) and its implications for the origin of comets. *Icarus* 133: 147-162
- 38 Meier M, Owen TC, Matthews HE, Jewitt DC, Bockelée-Morvan D, Biver N, Crovisier J, Gautier D (1998) A determination of the HDO/H₂O ratio in comet C/1995 O1 (Hale Bopp). *Science* 279: 842-844
- 39 Kieffer HH, Jakosky BM, Snyder CW, Matthews MS (eds) (1992) Mars. University of Arizona Press, Tucson
- 40 Acuña MH and 19 colleagues (1998) Magnetic field and plasma observations at Mars: initial results of the Mars Global Surveyor mission. *Science* 279: 1676-1680
- 41 Acuña MH and 19 colleagues (1999) Global distribution of crustal magnetization discovered by the Mars Global Surveyor MAG/ER experiment. *Science* 284: 790-793
- 42 Schubert G, Russell CT, Moore WB (2000) Timing of the Martian dynamo. *Nature* 408: 666-667
- 43 Weiss BP, Vali H, Baudenbacher FJ, Kirschvink JL, Stewart ST, Shuster DL (2002) Records of an ancient Martian magnetic field in ALH84001. *Earth Planet. Sci. Lett.* 201: 449-463
- 44 Cisowski SM (1986) Magnetic studies on Shergotty and other SNC meteorites. *Geochim. Cosmochim. Acta* 50: 1043-1048
- 45 Anderson Jr. DE, Hord CW (1971) Mariner 6 and 7 ultraviolet spectrometer experiment: analysis of hydrogen Lyman-Alpha data. *J. Geophys. Res.* 76: 6666-6673
- 46 Krasnopolsky VA, Feldman PD (2001) Detection of molecular hydrogen in the atmosphere of Mars. *Science* 294: 1914-1917
- 47 Lundin R, Dubinin EM, Koskinen H, Norberg O, Pissarenko N, Barabash SW (1991) On the momentum transfer of the solar wind to the Martian topside ionosphere. *Geophys. Res. Lett.* 18: 1059-1062
- 48 Spreiter JR, Stahara SS (1980) Solar wind flow past Venus: theory and comparisons. *J. Geophys. Res.* 85: 7715-7738
- 49 Lichtenegger HIM, Dubinin EM (1998) Model calculations of the planetary ion distribution in the Martian tail. *Earth Planets Space* 50: 445-452
- 50 Zhang MHG, Luhmann JG, Bougher SW, Nagy AF (1993) The ancient oxygen atmosphere of Mars: implications for atmosphere evolution. *J. Geophys. Res.* 98 (E6): 10915-10923
- 51 Leblanc F, Johnson RE (2002) Role of molecular species in pick up ion sputtering of the Martian atmosphere. *J. Geophys. Res.* 107(E2): 5010, 10.1029/2000JE001473
- 52 Lammer H, Lichtenegger HIM, Kolb C, Ribas I, Bauer SJ (2003) Loss of water from Mars: implications for the oxidation of the soil. *Icarus* 165: 9-25
- 53 Elphic RC, Ershkovich AI (1984) On the stability of the ionopause of Venus. *J. Geophys. Res.* 89: 997-1002
- 54 Chandrasekhar S (1961) Hydrodynamic and Hydromagnetic Stability. Oxford University Press, New York
- 55 Wolff RS, Goldstein BE, Yeates CM (1980) The onset and development of Kelvin-Helmholtz instability at the Venusian ionopause. *J. Geophys. Res.* 85: 7697-7707
- 56 Brace LH, Theis RF, Hoegy WR (1982) Plasma clouds above the ionopause of Venus and their implications. *Planet. Space Sci.* 30: 29-37

-
- 57 Penz T, Erkaev NV, Lammer H, Amerstorfer UV, Biernat HK, Gunell H, Kallio E, Barabash S, Orsini S, Milillo A, Baumjohann W (2003) Ion loss on Mars caused by the Kelvin-Helmholtz instability. Submitted to Planet. Space Sci.
- 58 Pérez-de-Tejada H (1992) Solar wind erosion of the Mars early atmosphere. *J. Geophys. Res.* 97 (A3): 3159-3167
- 59 Pérez-de-Tejada H (1998) Momentum transport in the solar wind erosion of the Mars ionosphere. *J. Geophys. Res.* 103 (E13): 31499-31508
- 60 Amerstorfer UV (2004) Solar wind flow past Venus and Mars. Master's Thesis. University of Graz
- 61 Jakosky BM, Pepin RO, Johnson RE, Fox JL (1994) Mars atmospheric loss and isotopic fractionation by solar-wind induced sputtering and photochemical escape. *Icarus* 111: 271-288
- 62 McElroy MB (1972) Mars: an evolving atmosphere. *Science* 175: 443-445
- 63 Luhmann JG (1997) Correction to "The ancient oxygen exosphere of Mars: implications for atmospheric evolution". *J. Geophys. Res.* 102 (E1): 1637-1638
- 64 Nair H, Allen M, Anbar AD, Yung YL, Clancy RT (1994) A photochemical model of the Martian atmosphere. *Icarus* 111: 124-150
- 65 Flynn GJ, McKay DS (1990) An assessment of the meteoritic contribution to the Martian soil. *J. Geophys. Res.* 95(B9): 14497-14509
- 66 Kolb C, Abart R, Lammer H (2003) The meteoritic component on the surface of Mars: evidence for a global dust unit and implications for oxidation states of the Martian surface. Submitted to *Icarus*
- 67 Zent AP (1998) On the thickness of the oxidized layer of the Martian regolith. *J. Geophys. Res.* 103 (E13): 31491-31498
- 68 Carr MH (1981) *The Surface of Mars*. Yale University Press, New Haven
- 69 Neukum G, Ivanov BA (1994) Crater size distributions and impact probabilities on Earth from lunar, terrestrial-planet, and asteroid cratering data. In: Gehrels T (ed) *Hazards due to Comets and Asteroids*. University of Arizona Press, Tucson
- 70 Bell III JF, McSween Jr. HY, Crisp JA, Morris RV, Murchie SL, Bridges NT, Johnsen JR, Britt TD, Golombek MP, Moore HJ, Ghosh A, Bishop JL, Anderson RC, Brückner J, Economou T, Greenwood JP, Gunnlaugsson HP, Hargraves RM, Hviid S, Knudsen JM, Madsen MP, Reid R, Rieder R, Soderblom L (2000) Mineralogic and compositional properties of Martian soil and dust: results from Mars Pathfinder. *J. Geophys. Res.* 105(E1): 1721-1755
- 71 Yen AS, Kim SS, Hecht MH, Frant MS, Murray B (2000) Evidence that the reactivity of the Martian soil is due to superoxide ions. *Science* 289: 1909-1912
- 72 Patel MR, Bérces A, Kolb C, Lammer H, Rettberg P, Zarnecki JC, Selsis F (2003) Seasonal and diurnal variations in Martian surface UV irradiation: biological and chemical implications for the Martian regolith. *Int. J. Astrobiol.* 2: 21-34
- 73 Huguenin RL (1973) Photostimulated oxidation of magnetite I. Kinetics and alteration phase identification. *J. Geophys. Res.* 78: 8481-8493
- 74 Biemann K, Oró J, Toulmin III P, Orgel LE, Nier AO, Anderson DM, Simmonds PG, Flory D, Diaz AV, Rushneck DR, Billier JE, Lafleur AE (1977) The search for organic substances and inorganic volatile compounds in the surface of Mars. *J. Geophys. Res.* 82 (B28): 4641-4658
- 75 Oyama VI, Berdahl BJ (1977) The Viking Gas Exchange Experiment results from Chryse and Utopia surface samples. *J. Geophys. Res.* 82 (B28): 4669-4676
- 76 Lammer H, Kolb C, Penz T, Amerstorfer UV, Biernat HK, Bodiselitsch B (2003) Estimation of the past and present water-ice reservoirs by isotopic constraints on exchange between the atmosphere and the surface. *Int. J. Astrobiol.* 2: 195-202
- 77 Pollack JB (1979) Climatic change on the terrestrial planets. *Icarus* 37: 479-553